Journal of CO2 Utilization 81 (2024) 102735

Contents lists available at ScienceDirect

Journal of CO2 Utilization

journal homepage: www.elsevier.com/locate/jcou

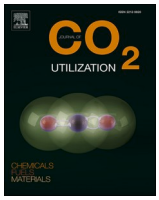

Exploring the impact of partial pressure and typical compounds on the continuous electroconversion of CO_2 into formate

Guillermo Díaz-Sainz *, José Antonio Abarca, Manuel Alvarez-Guerra, Angel Irabien

Departamento de Ingenierías Química y Biomolecular, Universidad de Cantabria, ETSIIyT, Avenida de Los Castros s/n, Santander 39005, Spain

ARTICLE INFO

Keywords:
CO_2 concentration
Gas compounds
Residence time
Electroreduction
Formate

ABSTRACT

Previous research in CO_2 electroreduction primarily focused on cathodic electrocatalysts and electrode configurations using pure CO_2. Few studies explored the impact of residence time and N_2/O_2 compounds, crucial for practical industrial implementation. In this study, the effect of residence time and the influence of N_2 and O_2 compounds on CO_2 electroreduction to formate are investigated, employing Bi carbon-supported nanoparticles in the form of Gas Diffusion Electrodes within an electrochemical flow reactor with a single pass of the reactants. The results highlight the critical role of residence time and the impact of N_2 and O_2 compounds in the CO_2 electroconversion process. On the one hand, the evaluation of residence time holds paramount significance for the potential establishment of a large-scale CO_2 recycling plant, as it has the potential to significantly impact both the capital and operational costs of the integrated electrolyzer-separator system. Optimal results are obtained in the range of residence times between 1.8 and 2.9 seconds, corresponding to CO_2 flow rates of 150 and 250 mL·min^{-1}, respectively. On the other hand, the study resulted in a promising Faradaic Efficiency for formate of 75.0%, with similar values achieved at CO_2 concentrations in the range of 75 – 100 vol%. These results are particularly noteworthy as they demonstrate that achieving a CO_2 capture efficiency of 100% is not necessary, thereby reducing the costs associated with this process and, consequently, the overall cost of integrating both capture and utilization processes in a CO_2 recycling plant.

1. Introduction

The World Meteorological Organization (WMO) recently reported that the concentration of carbon dioxide (CO_2) in the atmosphere exceeded 149% of the pre-industrial level in 2021. This increase can be predominantly attributed to emissions from fossil fuels and cement production [1]. Moreover, a primary objective outlined at the UN Climate Change Conference of the Parties (COP27), held in Sharm el-Sheikh (Egypt), is to accomplish ambitious reductions in emissions by 2030, ultimately aiming to achieve net-zero emissions by the mid-21st century [2].

Consequently, there is a growing emphasis on the electrocatalytic reduction of CO_2 into value-added chemicals, driven by electrical renewable energy sources. This strategy has gained considerable attention and is considered a promising approach to mitigate the impacts of climate change [3–5]. Remarkable progress has been made in the field of CO_2 electroreduction, encompassing the development of catalysts [6,7], reactor configurations [8–10], and optimization of operating parameters [11,12]. These advancements have led to high Faradaic Efficiencies (FEs) for specific products, such as formate/formic acid [13], carbon monoxide (with FEs exceeding 90%) [14], methane [15,16], hydrocarbons [17,18], acetate [19] and formaldehyde (with FEs ranging between 70% and 80%), as well as alcohols (with FEs approximately around 60%) [20].

However, it is noteworthy that the current Technological Readiness Level (TRL) for this process generally falls within the range of 3–5 [18], indicating that significant progress is required before reaching industrial scale-up implementation. It is important to highlight that much of the research in the field of continuous electrochemical CO_2 reduction to produce chemicals relies on utilizing a pure CO_2 gaseous stream in the cathode chamber of the electrochemical reactor [12,21,22]. This assumption is based on the expectation that these pure CO_2 sources will be obtained from forthcoming, energy-intensive capture technologies [23].

Among the various products that can be derived from CO_2 reduction, formate holds significant importance as a widely utilized chemical commodity in various industries, including pharmaceutical and leather processing [24,25]. Additionally, formate can serve as a fuel source,

* Corresponding author.
E-mail address: diazsg@unican.es (G. Díaz-Sainz).

https://doi.org/10.1016/j.jcou.2024.102735
Received 12 December 2023; Received in revised form 29 January 2024; Accepted 11 March 2024
Available online 19 March 2024

even when starting from relatively low concentrations (as low as 0.5 M in solution), for direct formate fuel cells (DFAFCs), enabling electricity generation. It is worth noting that formate ranks among the most valuable CO_2 conversion products in terms of market price, with this chemical having a market value ranging from approximately $1000 to $1700 per ton of product [26].

In this context, a limited number of studies [27–50] have been conducted to investigate the influence of CO_2 concentration on the production of value-added products. This research encompassses efforts to reduce the CO_2 partial pressure in the input stream [51] and the consideration of various impurities and other non-CO_2 compounds within the input stream in recent years. Among these impurities, it is important to include sulfur dioxide (SO_2) [27,29,35,36,40–43], nitric oxide (NO) [27,30,35,40,41,47], nitrogen Dioxide (NO_2) [30,36,42,43,52], nitrous oxide (N_2O) [30], water (H_2O) [36], carbon monoxide (CO) [36], particulate matter [36], and hydrocarbons [36]. Besides, oxygen (O_2) [31–33,35–37,41,44,48,50] and nitrogen (N_2) [28,34,36,38,39,44–46,49], which appear in higher concentrations, also have the potential to significantly impact the performance of CO_2 electrolyzers.

Utilizing CO_2 directly from the flue gas point sources is of immense economic interest, as it eliminates the need for capture and purification steps. However, understanding the effects of impurities and other compounds during CO_2 electrolysis is crucial for the practical application of this technology.

Table 1 compiles a selection of studies from the literature spanning the years 2015–2023 that investigate the impact of impurities and other compounds in the gaseous input stream. This table provides information about the working electrode, the target product achieved, the supplied current density, and the specific type of impurities and other components introduced, within the field of CO_2 electroreduction for the production of value-added products.

In the context of formic acid or formate production through CO_2 electroreduction, there is a limited number of studies that specifically investigate the effects of these impurities and compounds. Most of these studies have predominantly focused on the utilization of Sn-based cathodes [27–30,32] to generate formic acid or formate as the desired product in the CO_2 electroreduction process.

For instance, Choi et al. [27]conducted CO_2 electrolysis experiments using diluted streams containing 15 vol% CO_2 (equivalent to a partial pressure of 0.15 atm.) with SO_2 and NO impurities, achieving notable performances. On a different note, Van Daele et al. [28] successfully operated a continuous flow cell with a less concentrated gaseous stream (60 vol% CO_2 or CO_2 partial pressure of 0.6 atm) at current densities of up to 300 $mA{\cdot}cm^{-2}$, comparing the production of formate on SnO_2 catalysts. Furthermore, Luc et al., [29] studied the effects of SO_2 on Sn-catalyzed CO_2 electrolysis in a flow-cell electrolyzer, while Ko et al., [30] investigated the impact of various nitrogen oxides, including NO, NO_2, and N_2O, on carbon dioxide electroreduction using tin electrocatalysts. In addition, Li et al., [32] explored the influence of O_2 on the electrochemical conversion of CO_2 into formate, demonstrating the potential for the direct electrocatalytic conversion of flue gas CO_2 streams.

Specifically, research efforts for the CO_2 electroreduction to formic acid and formate have thus far concentrated on the development of cathodic electrocatalysts [53–55], with an emphasis on Bi-based catalysts [56–58]. Regarding the influence of these compounds in these studies and as summarized in Table 1, only two studies have reported the use of Bi-based cathodes for the CO_2 electroreduction to formic acid and formate, studying the effect of these compounds in the input stream [34,35]. Yang et al., [34] introduced a surface oxygen modulation strategy to develop efficient Bi_2O_3 catalyst for directly reducing commercially relevant flue gas into valuable chemicals. They achieved a maximum Faradaic Efficiency of 97.3% in simulated flue gas (comprising 15% CO_2 balanced by nitrogen with trace impurities),

Table 1
Summary of experimental conditions and results in the literature investigating impurities and non-CO_2 components in the gaseous input stream for the electrocatalytic reduction of CO_2 to produce value-added products.

Working electrode	Target product	Impurities and other compounds	Current density ($mA{\cdot}cm^{-2}$)	Faradaic Efficiency (%)	Year	Reference
Ag-GDE	CO	N_2	36.2	>80	2015	[39]
CoPc/CNT electrode	CO	O_2	27.3	75.9	2019	[31]
Ag, Sn and Cu electrodes	CO (Ag), formate (Sn) and CO, formate and C_2+ (Cu)	SO_2	100	>80	2019	[29]
Cu-PTFE GDE	C_2	O_2	< 300	68	2020	[33]
Co-phthalocyanine-based cathode / Sn-electrode	CO (Co) and formate (Sn)	O_2	56.7	71 (CO) and 100 (formate)	2020	[32]
Cu, Ag and Sn electrodes	C_2+ (Cu), CO (Ag) and formate (Sn)	NO, NO_2, N_2O	100	25.9 (C_2^+), 34.5 (CO) and 9.1 (formate)	2020	[30]
Cu cathodes	CH_4, CO and formate	O_2	>100	8.2 (CH_4), 1.66 (CO) and 2.1 (formate)	2020	[50]
Sn-GDE	Formate	N_2	>100	>70	2021	[27]
Ag	CO	N_2		40	2021	[38]
Ag-GDE SnO_2-GDE	CO (Ag) and formate (SnO_2)	N_2	300	>70 (formate)	2022	[28]
Pb	Methyl formate	SO_2, NO and O_2	18.5	<45	2022	[40]
Ni-N-C electrode	CO	NO_x, SO_2 and VOC	470	99	2022	[43]
MOF-based GDE	CO	N_2 and O_2	30*	95	2022	[44]
Ag-GDE	CO	N_2	250	>78	2022	[45]
In-SSZ-13	Formate	N_2	133.3*	92	2022	[46]
Pd@Cu	CO	NO	(-)	(-)	2022	[47]
Bi_2O_3-GDE	Formate	N_2	205.5 (-1.3 V)	>90	2023	[34]
Gas-fed liquid-covered electrodes	Formate	N_2 and O_2	3.0	70	2023	[37]
Ag foam and Ni foam	CO	NO_x and SO_x	400	<5	2023	[42]
Cu/P-GDL	C_2^+	O_2	132*	44.8 (C_2H_4), and 19 (C_2H_5OH)	2023	[48]
Cu cathode	C_2H_4	N_2	80	45	2023	[49]
Ag-GDE Bi_2O_3-GDE	CO (Ag) and formate (Bi_2O_3)	SO_2, NO and O_2	300	>90	2024	[35]

* Partial current density value reported.
(-) Figures of merit are not reported.

primarily for formate production. In contrast, Van Daele et al. [35] demonstrated efficient performance with commercial Bi_2O_3 nanoparticles, with a Faradaic Efficiency exceeding 90%, along with stability over a 20-hour period when exposed to 200 ppm of SO_2 or NO in the feed gas stream.

Thus, there is limited knowledge regarding the impact of impurities and other components on Bi-based electrodes for CO_2 electroreduction to formic acid and formate. Among the different electrode configurations, Gas Diffusion Electrodes (GDEs) stand out for their ability to enhance performance by facilitating improved contact between the reactive gas, the catalyst, and the electrolyte [59].

All in all, this study aims to examine the influence of N_2 and O_2 compounds on the CO_2 electroreduction to formate, using Bi carbon-supported nanoparticles in the form of Gas Diffusion Electrodes (Bi-GDEs) within an electrochemical flow reactor with a single pass of the reactants. These Bi-cathodes allow us to achieve one of the best trade-offs reported in the literature to date for CO_2 electroreduction to formate [12]. The objective of this research is to advance this process and bring it closer to industrial-scale implementation, particularly when integrated with CO_2 capture methods. Additionally, the investigation explores the impact of residence time, which has been scarcely explored yet, within the cathodic compartments. This residence time is controlled by adjusting the feed flow rate to enhance formate selectivity, and promising results have been obtained in terms of formate concentration, Faradaic Efficiency, rate, and energy consumption.

2. Methodology

2.1. Experimental setup for CO_2 flow electrolyzer

All experiments related to the continuous electrocatalytic reduction of CO_2 to formate, as detailed in this manuscript, were conducted using a filter press reactor within the experimental laboratory system depicted in Fig. 1.

The experiments were carried out using a liquid feed at the cathode side of the filter-press reactor, a configuration that has been extensively investigated in prior studies, enabling a reliable comparison with previous approaches [60,61]. Electrochemical experiments were conducted in duplicate, with an operating time of 60 minutes, under ambient temperature and pressure conditions.

Two magnetically stirred glass tanks were used as reservoirs for the catholyte and the anolyte. Specifically, a 0.45 M $KHCO_3$ + 0.5 M KCl aqueous solution was employed as the catholyte, while a 1 M KOH solution served as the anolyte. Both electrolytes were circulated independently through their respective compartments, passing through the reactor once, using peristaltic pumps (Watson Marlow 320, Watson Marlow Pumps Group) with a constant flow rate per geometric surface area of 0.57 $mL{\cdot}min^{-1}cm^{-2}$. Furthermore, experiments were conducted under galvanostatic conditions using a potentiostat-galvanostat (Arbin Instruments, MSTAT4) with a current density of 90 $mA{\cdot}cm^{-2}$.

As illustrated in Fig. 1, the primary component of the experimental setup is the electrochemical reactor (Micro Flow Cell, ElectroCell A/S). Fig. 2 provides a schematic representation of the filter press reactor configuration, consisting of two compartments separated by a Nafion 117 cationic-exchange membrane. The working electrode was a Bi Gas Diffusion Electrode (Bi-GDE), while a dimensionally stable anode, DSA/O_2(Ir-MMO mixed metal oxide on platinum), was employed as a counter electrode, as elaborated in the following subsections. Both electrodes possessed an active area of 10 cm^2. A leak-free Ag/AgCl 3.4 M KCl reference electrode was positioned within a PTFE frame in the cathodic compartment of the filter press reactor.

Samples were taken from the outlet stream on the cathode side of the electrochemical reactor at various time intervals (20, 40 and 60 min), and the average formate concentration was determined for each experiment. Ion chromatography (Dionex ICS 1100) equipped with an AS9-HC column was used to analyze this concentration.

2.2. Working electrode configuration

A Bi-GDE was selected as the working electrode for the CO_2 electroreduction to formate. The GDE configuration consists of three distinct layers, illustrated in Fig. 3: the carbonaceous support, the microporous layer (MPL) and the catalytic layer (CL).

The carbonaceous support employed in this study was Toray Carbon Paper TGP-H-60 (Alfa Aesar). The MPL, applied using an air-brushing technique, was formulated using Vulcan XC-72R and PTFE (Polytetrafluoroethylene preparation, 60 wt% dispersion in H_2O, Sigma-Aldrich) in a 40–60 wt% ratio, following a previously established method [11,12,60,61]. Subsequently, this layer underwent sintering at 623 K in a muffle furnace (PR series, Hobersal) for a duration of 30 minutes.

The catalytic ink for the GDE consisted of Bi carbon-supported nanoparticles, which served as the electrocatalyst, along with Nafion and isopropanol. The composition of these components matched that used in previous studies [11,12,60,61]. This ink was sonicated for approximately 30 minutes and then applied until a Bi loading of 0.75 $mg{\cdot}cm^{-2}$ was achieved. The loading level is considered optimal for performance.

The synthesis and characterization of the Bi carbo-supported

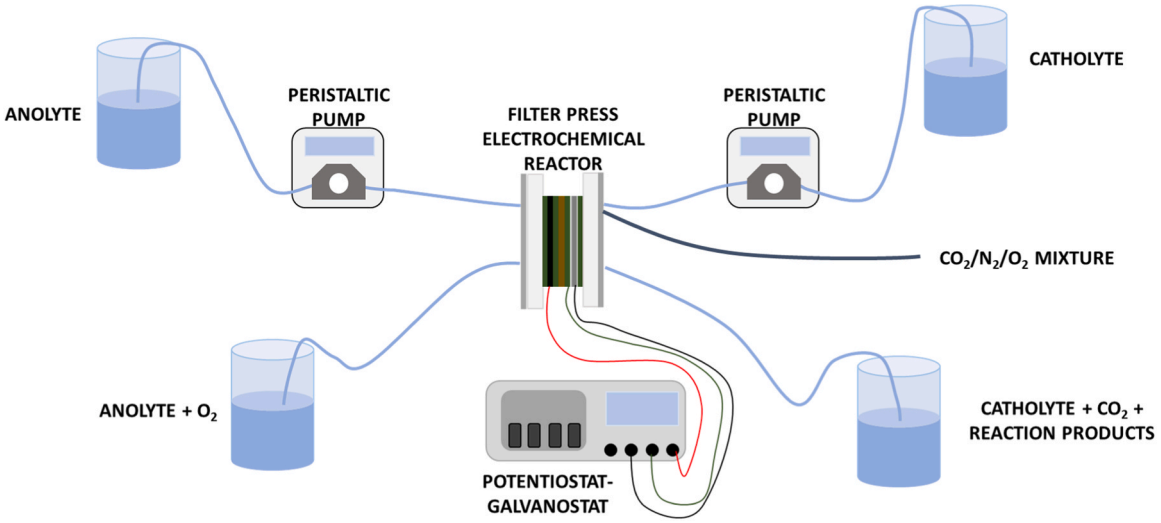

Fig. 1. Experimental setup employed for the continuous electrocatalytic reduction of CO_2 to formate in a filter press reactor.

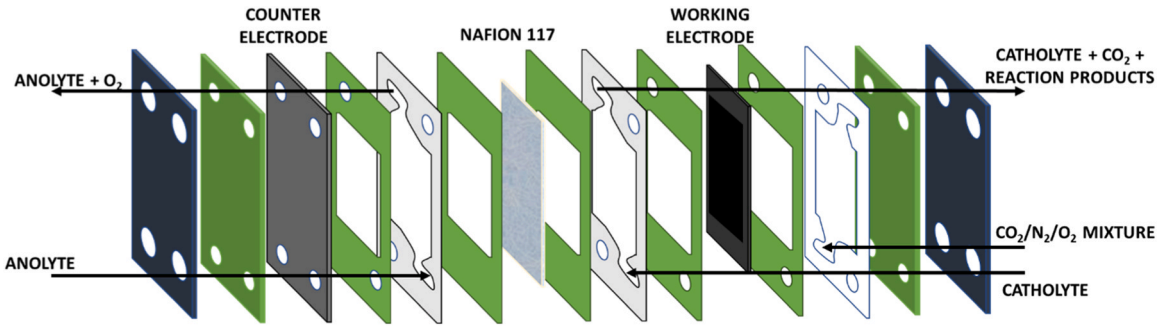

Fig. 2. Filter press reactor configuration employed for the continuous electrocatalytic reduction of CO_2 to formate in a filter press reactor.

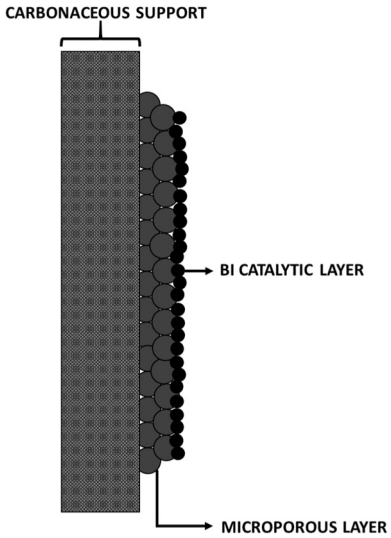

Fig. 3. Composition of the cathode side GDE comprising: (i) carbonaceous support, (ii) microporous layer, and (iii) Bi catalytic layer.

nanoparticles involved the use of $BiCl_3$ as a precursor and Vulcan XC-72R as the carbon support [58]. Furthermore, the Bi/C-GDE has undergone characterization in earlier research conducted by the research group [12,60].

2.3. Experimental conditions for the CO_2 input stream

To study the influence of residence time, a range of pure CO_2 flow rates, ranging from 50 to 400 mL·min^{-1}, was introduced into the cathodic compartment of the flow reactor. The residence time within the cathodic compartment was determined by measuring and estimating the dimensions and internal volumes of all components inside the electrochemical reactor (Figure S1, S2 and S3 of the Supporting Information). Once the volume of the cathodic compartment was calculated (7.36 mL), the residence time was determined by considering the relationship between the volume of the cathodic compartment and the CO_2 flow rate, which is the variable studied in the process.

Furthermore, the performance of the CO_2 electroreduction to formate process was assessed under various compositions of CO_2, N_2 and O_2 in the feed stream on the cathode side of the electrochemical reactor. The specific experimental conditions are detailed in Table 2, with a consistent total flow rate of 250 mL·min^{-1} maintained throughout the experiments.

2.4. Figures of merit

In each experiment, an average value of formate was determined to calculate the Faradaic Efficiency towards formate, the formate rate, and the energy consumption per kilomole of formate.

Table 2
Composition of CO_2, N_2, and O_2 (vol%) in the feed stream on the cathode side of the electrochemical reactor (total flow rate of 250 mL·min^{-1}).

Point	CO_2 concentration (vol %)	N_2 concentration (vol %)	O_2 concentration (vol %)
1	100	0	0
2	90	10	0
3	75	25	0
4	65	35	0
5	55	45	0
6	50	50	0
7	40	60	0
8	28	72	0
9	18	82	0
10	75	19.75	5.25
11	60	31.60	8.40
12	50	39.50	10.50

The Faradaic Efficiency (%) for the target product represents the percentage of the total current density supplied to the electrochemical filter press that contributed to the production of the desired product. This can be calculated using Eq. (1):

$$FE = \frac{z \cdot M \cdot F}{j \cdot A} \quad (1)$$

Where, z represents the number of electrons exchanged during the electrochemical conversion of CO_2 to value-added products (typically 2 electrons for the reduction of CO_2 to formate), M denotes the number of moles of the target product generated, F stands for the Faraday constant (96,485 C·mol^{-1}), j signifies the current density supplied to the electrochemical filter press and A represents the geometric electrode area.

The formate rate (mol·m^{-2}·s^{-1}) measures the quantity of the target product produced per unit of cathode area and unit of time and can be calculated using Eq. (2):

$$Rate = \frac{M}{t \cdot A} \quad (2)$$

Where, M and A are also the number of moles of the target product generated and the geometric electrode area, respectively, while t represents the duration of each experiment.

Furthermore, the energy consumption per kilomole of formate (kWh·kmol^{-1}) is defined as the amount of energy required to produce the desirable product and can be calculated as follows using Eq. (3).

$$\text{Energy consumption} = \frac{j \cdot A \cdot V}{M} \quad (3)$$

where j, A and M are, once again, the current density supplied to the electrochemical filter press cell, the geometric electrode area and the number of moles of the target product generated, respectively, and V

represents the cell potential of the electrochemical filter press during each experiment.

3. Results and discussion

3.1. Effect of the residence time

The electrocatalytic reduction of CO_2 to formate was examined in continuous mode using a filter press reactor with a liquid electrolyte at the cathode side, with an aqueous 1 M KOH solution serving as the anolyte. A Nafion cation exchange membrane was used to separate the anodic and cathodic compartments. The influence of residence time on the electrochemical reduction of CO_2 using Bi-based cathodes in a two-compartment cell configuration is examined. Experiments were conducted across a range of residence times, spanning from 1.1 to 8.8 seconds (equivalent to pure CO_2 flow rates in the input stream ranging from 50 to 400 mL·min^{-1}). To determine residence time, the dimensions of all components within the electrochemical reactor were determined using the AutoCAD tool. In the cathodic compartment, where the CO_2 flow rate plays a crucial role, various frames and gaskets were utilized, and the dimensions of these components are detailed in the Supporting Information.

Fig. 4a illustrates the impact of residence time in the cathodic compartment of the electrochemical reactor on the Faradaic Efficiency for formate, while Fig. 4b depicts the effect of residence time on the formate rate (values are described in Table S1). A Faradaic Efficiency for formate of 85.2% and a formate rate of 3.98 mmol·m^{-2}·s^{-1} were achieved with a residence time of 1.8 seconds, corresponding to a pure CO_2 flow rate of 250 mL·min^{-1}.

However, increasing the residence time from 1.8 to 2.2 and 2.9 seconds yields the most favourable outcomes in terms of Faradaic Efficiency for formate and formate rate. Specifically, the Faradaic Efficiency increases from 85.2% to 95.1%, while the formate rate rises from 3.98 mmol·m^{-2}·s^{-1} to 4.44 mmol·m^{-2}·s^{-1}. These findings suggest that the optimal range of CO_2 flow rates for this electrochemical reactor, with a geometric area of 10 cm^2, falls between 150 and 250 mL·min^{-1}.

Although the decline in performance is less pronounced when the residence time is reduced to 1.1 and 1.5 seconds, corresponding to a CO_2 flow rate of 300 and 400 mL·min^{-1}, the poorest results were obtained at the highest residence time values of 5.9 and 8.8 seconds. Operating at these residence times resulted in similar values of Faradaic Efficiency for formate, around 68%, and a formate rate of approximately 3.17 mmol·m^{-2}·s^{-1}.

Similar results were observed in Fig. 5, illustrating the influence of residence time on formate concentration (Fig. 5a) and energy consumption (Fig. 5b). Both formate concentration and energy consumption exhibited comparable trends. Notably, intriguing formate concentrations of approximately 2.0 g·L^{-1} were achieved with low energy consumption levels close to 200 kWh·kmol^{-1}. These results were observed within a residence time range of 1.8–2.9 seconds, corresponding to a CO_2 flow rate ranging from 250 to 150 mL·min^{-1} and a single-pass CO_2 conversion rates ranging from 2.1% to 3.9%, respectively.

The evaluation of residence time assumes paramount significance in the potential establishment of a large-scale CO_2 recycling plant, as it holds the potential to significantly impact both the capital and operational costs of the integrated electrolyzer-separator system. Moreover, the CO_2 flow rate plays a crucial role in determining single-pass conversion and product selectivity, particularly in the context of formate production.

In this context, enhancing single-pass conversion results in a greater

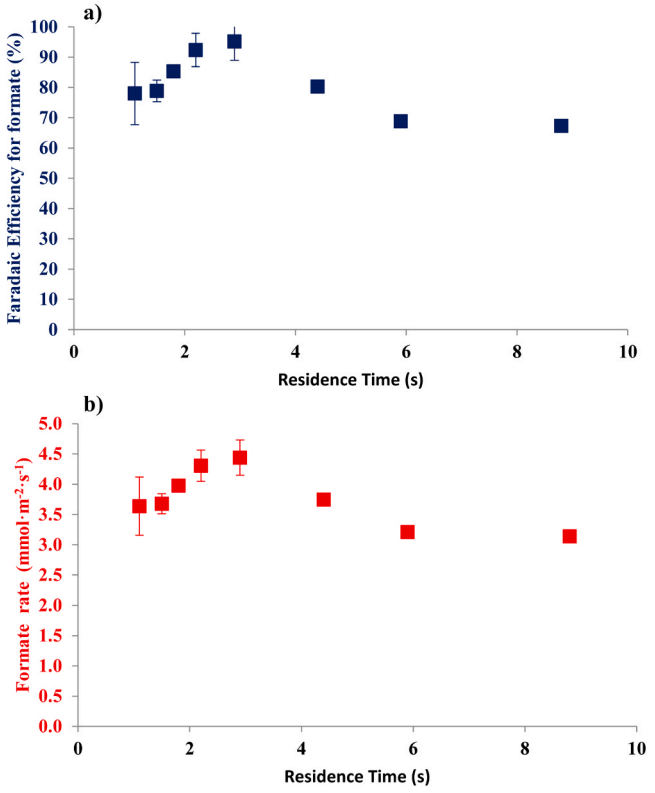

Fig. 4. Influence of residence time in the cathodic compartment of the electrochemical reactor on: a) Faradaic Efficiency for formate (%) and b) formate rate (mmol·m^{-2}·s^{-1}) in the residence time range of 1.1 – 8.8 s. The experiments were conducted at room temperature (20 °C), with a Bi Catalyst loading of 0.75 mg·cm^{-2}, electrolyte flow rates per geometric surface area of 0.57 mL·min^{-1}·cm^{-2}, and a current density of 90 mA·cm^{-2}.

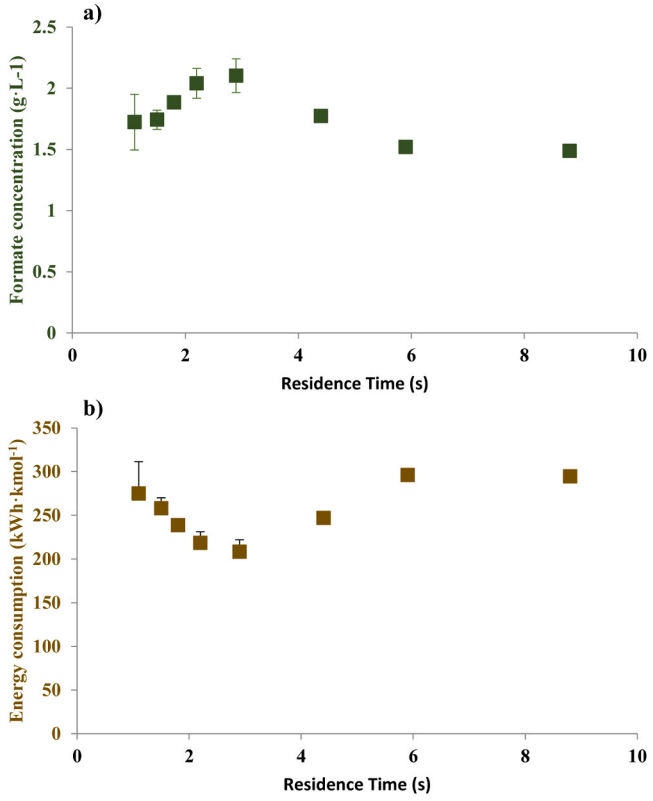

Fig. 5. Influence of residence time in the cathodic compartment of the electrochemical reactor on: a) formate concentration (g·L^{-1}) and b) energy consumption per kmol of formate (kWh·kmol^{-1}) in the residence time range of 1.1 – 8.8 s. The experiments were conducted at room temperature (20 °C), with a Bi Catalyst loading of 0.75 mg·cm^{-2}, electrolyte flow rates per geometric surface area of 0.57 mL·min^{-1}·cm^{-2}, and a current density of 90 mA·cm^{-2}.

disparity in CO_2 concentration between the inlet and outlet streams, leading to a lower CO_2 concentration in the cathode-side catalyst layer near the cell exit compared to that at the inlet. To address this, it is imperative to explore the CO_2 electroreduction to formate process to identify the optimal residence time concerning formate rate, Faradaic Efficiency, formate concentration, and energy consumption.

3.2. Impact of various CO_2 concentrations balanced by N_2 in the inlet gas stream

This section provides an overview of experiments with CO_2 concentrations in the input stream ranging from 18 to 100 vol%, balanced by N_2. The experiments involved a Bi catalyst loading of 0.75 mg·cm^{-2}, electrolyte flow rates per geometric surface area of 0.57 mL·min^{-1}·cm^{-2}, and a total gaseous flow rate of 250 mL·min^{-1}, considered the optimal value in the previous section. Notably, the gaseous input stream exclusively comprised CO_2, with N_2 as the sole impurity.

As shown in Fig. 6, the influence of CO_2 concentration in the input stream on the Faradaic Efficiency for formate and the formate rate is depicted. Detailed values for all experiments can be found in Table S2 of the Supplementary Information. Initially, working with CO_2 concentrations below 40 vol%, and even at a concentration of 40 vol%, resulted in negligible values for Faradaic Efficiency for formate and formate rate. However, increasing the CO_2 concentration in the input stream from 40 to 65 vol% led to a thirteenfold increase in the Faradaic Efficiency for formate, reaching 63.9% at a CO_2 concentration of 65 vol%. These results suggest minimal negative influence of CO_2 concentration below 50 vol%. Working with CO_2 concentrations of 75 vol% resulted in a promising Faradaic Efficiency for formate of 75.0%, with similar values achieved at CO_2 concentrations in the range of 90 – 100 vol%. Regarding the formate rate, operating with CO_2 concentrations of 75 and 90 vol% led to an approximately 66% increase (3.5 mmol·m^{-2}·s^{-}1) and a 90% (4.0 mmol·m^{-2}·s^{-1}) when compared to the CO_2 concentration of 50 vol %.

The concentration of the product of interest follows the same trend as the Faradaic Efficiency and formate rate mentioned previously, as depicted in Fig. 7 (detailed values provided in Table S1 of the Supporting Information). A maximum formate concentration of approximately 1.9 g·L^{-1} was obtained in the CO_2 concentration range from 90 to 100 vol%, resulting in a single-pass CO_2 conversion rate of approximately 2.2%. These results are particularly noteworthy as they demonstrated that achieving a CO_2 capture efficiency of 100% is not necessary, thereby reducing the costs associated with this process and, consequently, the overall cost of integrating both capture and utilization processes in a CO_2 recycling plant.

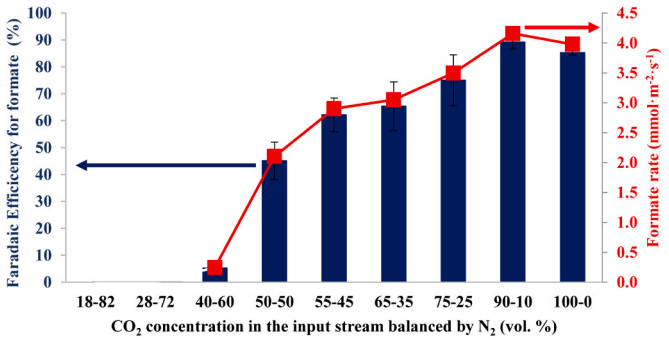

Fig. 6. Influence of CO_2 concentration in the input stream (vol%) (balanced by N_2) on the Faradaic Efficiency (%) and formate rate (mmol·m^{-2}·s^{-1}) in the CO_2 concentration range of 18% – 100%. The experiments were conducted at room temperature (20 °C), with a Bi Catalyst loading of 0.75 mg·cm^{-2}, electrolyte flow rates per geometric surface area of 0.57 mL·min^{-1}·cm^{-2}, a current density of 90 mA·cm^{-2}, and a total gaseous flow rate of 250 mL·min^{-1}.

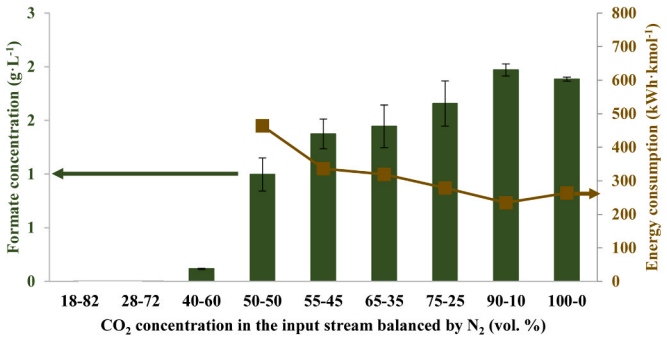

Fig. 7. Influence of CO_2 concentration in the input stream (vol%) (balanced by N_2) on the formate concentration (g·L^{-1}) and energy consumption (kWh·kmol^{-1}) in the CO_2 concentration range of 18% – 100%. The experiments were conducted at room temperature (20 °C), with a Bi Catalyst loading of 0.75 mg·cm^{-2}, electrolyte flow rates per geometric surface area of 0.57 mL·min^{-1}·cm^{-2}, a current density of 90 mA·cm^{-2}, and a total gaseous flow rate of 250 mL·min^{-1}.

Furthermore, it is important to emphasize that energy consumptions of less than 300 kWh·kmol^{-1} were achieved for CO_2 concentrations in the range from 75 to 100 vol% (specifically, values of only 279, and 264 kWh·kmol^{-1}, respectively). These exceptionally low energy consumptions can be attributed to the substantial amounts of formate achieved under all operating conditions.

These results align with findings in the existing literature that study the input of CO_2 and N_2 to the electrochemical reactor [27,28,34,37,46]. For example, Choi et al., [27] observed a decrease in Faradaic Efficiency for formate when using a CO_2 partial pressure below 0.5 atm, a pattern similar to the one observed in this study. Under such conditions, the carbonation reaction may exert a dominant influence in restricting CO_2 reactants when flow conditions are suboptimal. Furthermore, Van Daele et al., [28] proposed that reducing the composition of the CO_2 leads to a decreased current density response when using SnO_2-based cathodes for formate production. This behaviour was attributed to the interplay between partial pressure and CO_2 mass transport limitations, especially under atmospheric pressure conditions.

Yang et al., [34], investigated the electroreduction of CO_2 using simulated flue gas, with CO_2 concentrations ranging from 10% to 30%, balanced with N_2. Their results closely matched those obtained with pure CO_2, but a slight decrease in current density and Faradaic Efficiency was observed when a 15% CO_2 feeding gas was used. In another study, Takeda et al., [37] reported that reducing the CO_2 concentration led to an insufficient supply rate of CO_2 to the cathode electrode, resulting in a reduction in the Faradaic Efficiency of the target CO_2 reduction reaction.

Furthermore, when In-SSZ-3 catalysts were employed for CO_2 electroreduction to formate [46], a significant drop in performance was observed as the CO_2 concentration decreased from 50% to 60–20% CO_2. The excess of N_2 compound could adversely affect the catalysts and cells due to the low solubility of N_2 in the electrolyte, leading to the formation of gas bubbles. These gas bubbles, in turn, could adhere to the catalyst surface, potentially reducing the overall active surface area, or become trapped on the cationic exchange membrane, thereby limiting the ionic conductivity and affecting cell performance [36].

3.3. Influence of varied CO_2 concentrations balanced by N_2 and O_2 in the inlet gas stream

After assessing the behaviour of the electrochemical CO_2 reduction to formate process with the inlet gas stream composed of CO_2 and N_2, this section investigates the performance of the process under the influence of CO_2 concentration in the input stream, which is balanced with N_2 and O_2, as summarized in Table 2. Oxygen, being abundant in the

atmosphere and crucial for combustion processes that generate CO_2, has been incorporated into the study. The operating conditions remained consistent with those of the previous section, with ambient temperature (20ºC) and pressure (1 atm). The setup included a Bi catalyst loading of 0.75 mg·cm^{-2}, electrolyte flow rates per geometric surface area of 0.57 mL·min^{-1}·cm^{-2} and a total gaseous flow rate of 250 mL·min^{-1}.

Fig. 8 illustrates the impact of CO_2 concentration in the input stream, balanced by N_2 and O_2, on Faradaic Efficiency towards formate and formate rate (values are described in Table S3). When working with a mixture containing 75% CO_2, 19.75% N_2 and 5.25% O_2 in the input stream, similar results for Faradaic Efficiency (84.1%) and rate (3.9 mmol·m^{-2}·s^{-1}) were achieved compared to the results obtained with a stream composed solely of CO_2 and N_2, as discussed in the previous section.

Nevertheless, decreasing the CO_2 concentration from 75 to 60 vol%, while simultaneously increasing the N_2 and O_2 concentrations from 19.75 to 31.6 vol% and from 5.25 to 8.4 vol%, respectively, resulted in decreased performance in terms of Faradaic Efficiency and formate rate. Specifically, when operating with a stream containing 60% CO_2, 31.6% N_2 and 8.4% O_2, the Faradaic Efficiency and rate dropped to 39.8% and 1.8 mmol·m^{-2}·s^{-1}, respectively. These values were lower than the results obtained in the previous section, even when using CO_2 concentrations as low as 55 vol%.

Furthermore, when working with a stream containing 50% CO_2, 39.5% N_2 and 10.5% O_2, negligible values of Faradaic Efficiency for formate (1.4%) and rate (0.07 mmol·m^{-2}·s^{-}1) were achieved. This demonstrates that working with higher CO_2 concentrations in the input stream and lower concentrations of N_2 and O_2 has little influence on the performance of the CO_2 electroreduction to obtain the formate in terms of all the figures of merit.

However, increasing the concentration of O_2 in the input stream (10.5% O_2) negatively impacts the process's performance due to the competitive oxygen reduction reaction over the cathode surface. Recent studies [35] have shown that even the addition of just 1% O_2 to the CO_2 feed leads to a significant drop in Faradaic Efficiency for C-products. This is because the oxygen reduction reaction can occur under reducing potentials and is thermodynamically more favorable than CO_2 electroreduction to formate [62].

In terms of energy consumption and formate concentration, Fig. 9 demonstrates a comparable trend to that observed for Faradaic Efficiency and formate rate. Operating with a gas stream consisting of pure CO_2 and a mixture of 75% CO_2, 19.75% N_2 and 5.25% O_2 resulted in energy consumptions and concentrations for the target product of approximately 250 kWh·kmol^{-1} and 1.8 g·L^{-1}, respectively. This observation indicates that both performance figures of merit were negatively impacted by the decrease in CO_2 concentration and the

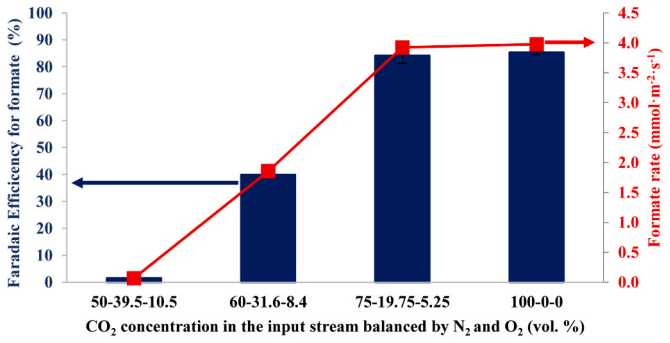

Fig. 8. Influence of CO_2 concentration in the input stream (vol%) (balanced by N_2 and O_2) on the Faradaic Efficiency (%) and formate rate (mmol·m^{-2}·s^{-1}) in the CO_2 concentration range of 50% – 100%. The experiments were conducted at room temperature (20 °C), with a Bi Catalyst loading of 0.75 mg·cm^{-2}, electrolyte flow rates per geometric surface area of 0.57 mL·min^{-1}·cm^{-2}, a current density of 90 mA·cm^{-2}, and a total gaseous flow rate of 250 mL·min^{-1}.

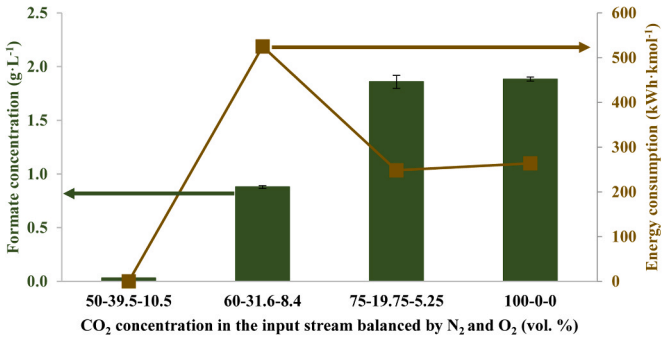

Fig. 9. Influence of CO_2 concentration in the input stream (vol%) (balanced by N_2 and O_2) on the formate concentration (g·L^{-1}) and energy consumption (kWh·kmol^{-1}) in the CO_2 concentration range of 50% – 100%. The experiments were conducted at room temperature (20 °C), with a Bi Catalyst loading of 0.75 mg·cm^{-2}, electrolyte flow rates per geometric surface area of 0.57 mL·min^{-1}·cm^{-2}, a current density of 90 mA·cm^{-2}, and a total gaseous flow rate of 250 mL·min^{-1}.

increase in N_2 and, notably, O_2 concentration.

This phenomenon can be attributed to the fact that the presence of O_2 promotes the oxygen reduction reaction. Recent studies suggest that these impurities could displace CO_2 reduction and consume up to 99% of the applied current in such systems [33]. Additionally, similar to N_2 compounds, the presence of O_2 bubbles could have detrimental effects by causing variations in cell voltage, oxidizing other metallic compounds within the cell, and affecting the oxidation of the generated products during CO_2 electroreduction, especially of formate in this study [36].

4. Conclusions

In this study, an assessment is conducted to evaluate the impact of residence time within the cathodic compartment of the electrochemical reactor and the influence of N_2 and O_2 compounds in the CO_2 input stream on the electroreduction of CO_2 to formate. The Bi-GDEs are tested in a continuous CO_2 electrolyzer, studying the influence of (i) residence time (ranging from 1.1 to 8.8 seconds or equivalent to pure CO_2 flow rates spanning from 50 to 400 mL·min^{-1}), and (ii) the CO_2 concentration in the input stream, balanced with N_2 and O_2.

On the one hand, the evaluation of residence time holds paramount significance for the potential establishment of a large-scale CO_2 recycling plant, as it has the potential to significantly impact both the capital and operational costs of the integrated electrolyzer-separator system. Optimal results are obtained in the range of residence times between 1.8 and 2.9 seconds, corresponding to CO_2 flow rate of 150 and 250 mL·min^{-1}, respectively. Although the decline in performance is less pronounced when the residence time is reduced to 1.1 and 1.5 seconds, corresponding to a CO_2 flow rate of 300 and 400 mL·min^{-1}, the poorest results were obtained at the highest residence time values of 5.9 and 8.8 seconds. Operating at these residence times resulted in similar values of Faradaic Efficiency for formate, around 68%, and a formate rate of approximately 3.17 mmol·m^{-2}·s^{-1}. Simultaneously, the CO_2 flow rate plays a crucial role in determining single-pass conversion and product selectivity, particularly in the context of formate production.

On the other hand, concerning the effect of the CO_2 concentration in the input stream, balanced by N_2 and O_2, it is important to highlight that working with CO_2 concentrations of 75 vol% resulted in a promising Faradaic Efficiency for formate of 75.0%, with similar values achieved at CO_2 concentrations in the range of 90 – 100 vol%. Regarding the formate rate, operating with CO_2 concentrations of 75 and 90 vol% led to an approximately 66% increase (3.5 mmol·m^{-2}·s^{-}1) and a 90% (4.0 mmol·m^{-2}·s^{-1}) when compared to the CO_2 concentration of 50 vol %. These results are particularly noteworthy as they demonstrate that

achieving a CO_2 capture efficiency of 100% is not necessary, thereby reducing the costs associated with this process and, consequently, the overall cost of integrating both capture and utilization processes in a CO_2 recycling plant. Thus, the results here reported represent a step forward in the field of CO_2 electroreduction to formate due to the advances in the study of these scarcely explored variables, bringing this process closer to future implementation at the industrial scale.

CRediT authorship contribution statement

José Antonio Abarca: Validation, Methodology, Investigation, Data curation, Conceptualization. **Manuel Alvarez-Guerra:** Writing – review & editing, Supervision, Project administration, Methodology, Funding acquisition, Conceptualization. **Angel Irabien:** Writing – review & editing, Supervision, Project administration, Funding acquisition. **Guillermo Díaz-Sainz:** Writing – original draft, Validation, Supervision, Methodology, Investigation, Data curation, Conceptualization.

Declaration of Competing Interest

The authors declare that they have no known competing financial interests or personal relationships that could have appeared to influence the work reported in this paper.

Data availability

No data was used for the research described in the article.

Acknowledgements

The authors fully acknowledge the financial support received from the Spanish State Research Agency (AEI) through the projects PID2020–112845RB-I00, TED2021–129810B-C21, and PLEC2022–009398 (MCIN/AEI/10.13039/501100011033 and Unión Europea Next Generation EU/PRTR). This project has received funding from the European Union's Horizon Europe research and innovation programme under grant agreement No 101118265. Jose Antonio Abarca gratefully acknowledges the predoctoral research grant (FPI) PRE2021–097200. We are also grateful for the Bi carbon-supported nanoparticles prepared and provided by the group of Prof. V. Montiel and Dr. José Solla-Gullón from the Institute of Electrochemistry of the University of Alicante.

Appendix A. Supporting information

Supplementary data associated with this article can be found in the online version at doi:10.1016/j.jcou.2024.102735.

References

[1] United States Environmental Protection Agency. https://www.epa.gov/ghgemissions/overview-greenhouse-gases#carbon-dioxide (Accessed 24 January 2024)
[2] Naciones Unidas. https://www.un.org/es/ (accessed January 24, 2024).
[3] Y.X. Duan, R.C. Cui, Q. Jiang, Recent progress on the electroreduction of carbon dioxide to C_1 liquid products, Curr. Opin. Electrochem. 38 (2023) 101219, https://doi.org/10.1016/j.coelec.2023.101219.
[4] Z. Yan, W. Liu, X. Liu, Z. Shen, X. Li, D. Cao, Recent progress in electrocatalytic conversion of CO_2 to valuable C_2 products, Adv. Mater. Interfaces 10 (2023) 2300186, https://doi.org/10.1002/admi.202300186.
[5] H. Wang, Z. Yu, J. Zhou, C. Li, A. Jayanarasimhan, X. Zhao, H. Zhang, A scientometric review of CO_2 electroreduction research from 2005 to 2022, Energies 16 (2023) 616, https://doi.org/10.3390/en16020616.
[6] M. Serafini, F. Mariani, F. Basile, E. Scavetta, D. Tonelli, From traditional to new benchmark catalysts for CO_2 electroreduction, Nanomaterials 13 (2023) 1723, https://doi.org/10.3390/nano13111723.
[7] X. Jiang, L. Lin, Y. Rong, R. Li, Q. Jiang, Y. Yang, D. Gao, Boosting CO_2 electroreduction to formate via bismuth oxide clusters, Nano Res. 16 (2022) 12050–12057, https://doi.org/10.1007/s12274-022-5073-0.
[8] J. Antonio Abarca, G. Díaz-Sainz, I. Merino-Garcia, A. Irabien, J. Albo, Photoelectrochemical CO_2 electrolyzers: from photoelectrode fabrication to reactor configuration, J. Energy Chem. 85 (2023) 455–480, https://doi.org/10.1016/j.jechem.2023.06.032.
[9] L. Yuan, S. Zeng, X. Zhang, X. Ji, S. Zhang, Advances and challenges of electrolyzers for large-scale CO_2 electroreduction, Mater. Rep.: Energy 3 (2023) 100177, https://doi.org/10.1016/j.matre.2023.100177.
[10] I. Merino-Garcia, E. Alvarez-Guerra, J. Albo, A. Irabien, Electrochemical membrane reactors for the utilisation of carbon dioxide, Chem. Eng. J. 305 (2016) 104–120, https://doi.org/10.1016/j.cej.2016.05.032.
[11] G. Díaz-Sainz, M. Alvarez-Guerra, A. Irabien, Continuous electroreduction of CO_2 towards formate in gas-phase operation at high current densities with an anion exchange membrane, J. CO_2 Util. 56 (2022) 101822, https://doi.org/10.1016/j.jcou.2021.101822.
[12] G. Díaz-Sainz, M. Alvarez-Guerra, B. Ávila-Bolívar, J. Solla-Gullón, V. Montiel, A. Irabien, Improving trade-offs in the figures of merit of gas-phase single-pass continuous CO_2 electrocatalytic reduction to formate, Chem. Eng. J. 405 (2021) 126965, https://doi.org/10.1016/j.cej.2020.126965.
[13] K. Fernández-Caso, G. Díaz-Sainz, M. Alvarez-Guerra, A. Irabien, Electroreduction of CO_2: advances in the continuous production of formic acid and formate, ACS Energy Lett. 8 (2023) 1992–2024, https://doi.org/10.1021/acsenergylett.3c00489.
[14] D. Wu, F. Jiao, Q. Lu, Progress and understanding of CO_2/CO electroreduction in flow electrolyzers, ACS Catal. 12 (2022) 12993–13020, https://doi.org/10.1021/acscatal.2c03348.
[15] S. Chen, Z. Zhang, W. Jiang, S. Zhang, J. Zhu, L. Wang, H. Ou, S. Zaman, L. Tan, P. Zhu, E. Zhang, P. Jiang, Y. Su, D. Wang, Y. Li, Engineering water molecules activation center on multisite electrocatalysts for enhanced CO_2 methanation, J. Am. Chem. Soc. 144 (2022) 12807–12815, https://doi.org/10.1021/jacs.2c03875.
[16] S. Chen, W.H. Li, W. Jiang, J. Yang, J. Zhu, L. Wang, H. Ou, Z. Zhuang, M. Chen, X. Sun, D. Wang, Y. Li, MOF encapsulating n-heterocyclic carbene-ligated copper single-atom site catalyst towards efficient methane electrosynthesis, Angew. Chem. - Int. Ed. 61 (2022) e202114450, https://doi.org/10.1002/anie.202114450.
[17] X. Chen, Y. Zhao, J. Han, Y. Bu, Copper-based catalysts for electrochemical reduction of carbon dioxide to ethylene, ChemPlusChem 88 (2023) e202200370, https://doi.org/10.1002/cplu.202200370.
[18] S. Chen, C. Ye, Z. Wang, P. Li, W. Jiang, Z. Zhuang, J. Zhu, X. Zheng, S. Zaman, H. Ou, L. Lv, L. Tan, Y. Su, J. Ouyang, D. Wang, Selective CO_2 reduction to ethylene mediated by adaptive small-molecule engineering of copper-based electrocatalysts, Angew. Chem. - Int. Ed. 62 (2023) e202315621, https://doi.org/10.1002/anie.202315621.
[19] H. Wang, J. Xue, C. Liu, Z. Chen, C. Li, X. Li, T. Zheng, Q. Jiang, C. Xia, CO_2 electrolysis toward acetate: a review, Curr. Opin. Electrochem. 39 (2023) 101253, https://doi.org/10.1016/j.coelec.2023.101253.
[20] S. Zhang, X. Jing, Y. Wang, F. Li, Towards carbon-neutral methanol production from carbon dioxide electroreduction, ChemNanoMat 7 (2021) 728–736, https://doi.org/10.1002/cnma.202100102.
[21] J. Albo, M. Perfecto-Irigaray, G. Beobide, A. Irabien, Cu/Bi metal-organic framework-based systems for an enhanced electrochemical transformation of CO_2 to alcohols, J. CO_2 Util. 33 (2019) 157–165, https://doi.org/10.1016/j.jcou.2019.05.025.
[22] C.A. Obasanjo, A.S. Zeraati, H.S. Shiran, T.N. Nguyen, S.M. Sadaf, M.G. Kibria, C. T. Dinh, In situ regeneration of copper catalysts for long-term electrochemical CO_2 reduction to multiple carbon products, J. Mater. Chem. A 10 (2022) 20059–20070, https://doi.org/10.1039/d2ta02709g.
[23] C. Kolster, E. Mechleri, S. Krevor, N. Mac Dowell, The role of CO_2 purification and transport networks in carbon capture and storage cost reduction, Int. J. Greenh. Gas. Control 58 (2017) 127–141, https://doi.org/10.1016/j.ijggc.2017.01.014.
[24] S.A. Al-Tamreh, M.H. Ibrahim, M.H. El-Naas, J. Vaes, D. Pant, A. Benamor, A. Amhamed, Electroreduction of carbon dioxide into formate: a comprehensive review, ChemElectroChem 8 (2021) 3207–3220, https://doi.org/10.1002/celc.202100438.
[25] A. Irabien, M. Alvarez-Guerra, J. Albo, A. Domínguez-Ramos, Electrochemical conversion of CO_2 to value-added products, in: C.A. Martínez-Huitle, M.A. Rodrigo, O. Scialdone (Eds.), Electrochemical Water Wastewater Treatmemt, Elsevier, 2019, pp. 29–59.
[26] I. Merino-Garcia, L. Tinat, J. Albo, M. Alvarez-Guerra, A. Irabien, O. Durupthy, V. Vivier, C.M. Sánchez-Sánchez, Continuous electroconversion of CO_2 into formate using 2 nm tin oxide nanoparticles, Appl. Catal. B: Environ. 297 (2021) 120447, https://doi.org/10.1016/j.apcatb.2021.120447.
[27] B.U. Choi, Y.C. Tan, H. Song, K.B. Lee, J. Oh, System design considerations for enhancing electroproduction of formate from simulated flue gas, ACS Sustain. Chem. Eng. 9 (2021) 2348–2357, https://doi.org/10.1021/acssuschemeng.0c08632.
[28] S. Van Daele, L. Hintjens, J. Van Den Hoek, S. Neukermans, N. Daems, J. Hereijgers, T. Breugelmans, Influence of the target product on the electrochemical reduction of diluted CO_2 in a continuous flow cell, J. CO_2 Util. 65 (2022) 102210, https://doi.org/10.1016/j.jcou.2022.102210.
[29] W. Luc, B.H. Ko, S. Kattel, S. Li, D. Su, J.G. Chen, F. Jiao, SO_2-Induced Selectivity Change in CO_2 Electroreduction, J. Am. Chem. Soc. 141 (2019) 9902–9909, https://doi.org/10.1021/jacs.9b03215.
[30] B.H. Ko, B. Hasa, H. Shin, E. Jeng, S. Overa, W. Chen, F. Jiao, The impact of nitrogen oxides on electrochemical carbon dioxide reduction, Nat. Commun. 11 (2020) 5856, https://doi.org/10.1038/s41467-020-19731-8.
[31] X. Lu, Z. Jiang, X. Yuan, Y. Wu, R. Malpass-Evans, Y. Zhong, Y. Liang, N. B. McKeown, H. Wang, A bio-inspired O_2-tolerant catalytic CO_2 reduction electrode, Sci. Bull. 64 (2019) 1890–1895, https://doi.org/10.1016/j.scib.2019.04.008.

[32] P. Li, X. Lu, Z. Wu, Y. Wu, R. Malpass-Evans, N.B. McKeown, X. Sun, H. Wang, Acid–base interaction enhancing oxygen tolerance in electrocatalytic carbon dioxide reduction, Angew. Chem. - Int. Ed. 59 (2020) 10918–10923, https://doi.org/10.1002/anie.202003093.
[33] Y. Xu, J.P. Edwards, J. Zhong, C.P. O'Brien, C.M. Gabardo, C. McCallum, J. Li, C. T. Dinh, E.H. Sargent, D. Sinton, Oxygen-tolerant electroproduction of C_2 products from simulated flue gas, Energy Environ. Sci. 13 (2020) 554–561, https://doi.org/10.1039/c9ee03077h.
[34] F. Yang, C. Liang, W. Zhou, W. Zhao, P. Li, Z. Hua, H. Yu, S. Chen, S. Deng, J. Li, Y. M. Lam, J. Wang, Oxide-Derived Bismuth as an Efficient Catalyst for Electrochemical Reduction of Flue Gas, Small 19 (2023) 2300417, https://doi.org/10.1002/smll.202300417.
[35] S. Van Daele, L. Hintjens, S. Hoekx, B. Bohlen, S. Neukermans, N. Daems, J. Hereijgers, T. Breugelmans, How flue gas impurities affect the electrochemical reduction of CO_2 to CO and formate, Appl. Catal. B: Environ. 341 (2024) 123345, https://doi.org/10.1016/j.apcatb.2023.123345.
[36] U. Legrand, U.P. Apfel, D.C. Boffito, J.R. Tavares, The effect of flue gas contaminants on the CO_2 electroreduction to formic acid, J. CO_2 Util. 42 (2020) 101315, https://doi.org/10.1016/j.jcou.2020.101315.
[37] Y. Takeda, S. Mizuno, R. Iwata, T. Morikawa, N. Kato, Gas-fed liquid-covered electrodes used for electrochemical reduction of dilute CO_2 in a flue gas, J. CO_2 Util. 71 (2023) 102472, https://doi.org/10.1016/j.jcou.2023.102472.
[38] D. Kim, W. Choi, H.W. Lee, S.Y. Lee, Y. Choi, D.K. Lee, W. Kim, J. Na, U. Lee, Y. J. Hwang, D.H. Won, Electrocatalytic reduction of low concentrations of CO_2 gas in a membrane electrode assembly electrolyzer, ACS Energy Lett. 6 (2021) 3488–3495, https://doi.org/10.1021/acsenergylett.1c01797.
[39] B. Kim, S. Ma, H.R. Molly Jhong, P.J.A. Kenis, Influence of dilute feed and pH on electrochemical reduction of CO_2 to CO on Ag in a continuous flow electrolyzer, Electro Acta 166 (2015) 271–276, https://doi.org/10.1016/j.electacta.2015.03.064.
[40] M. Gautam, D.T. Hofsommer, S.S. Uttarwar, N. Theaker, W.F. Paxton, C. A. Grapperhaus, J.M. Spurgeon, The effect of flue gas contaminants on electrochemical reduction of CO_2 to methyl formate in a dual methanol/water electrolysis system, Chem. Catal. 2 (2022) 2364–2378, https://doi.org/10.1016/j.checat.2022.08.001.
[41] C.A. Kong, R.R. Prabhakar, J.W. Ager, Electrochemical conversion of carbon dioxide to methyl formate with flue gas a Feedstock, Chem. Catal. 2 (2022) 2118–2139, https://doi.org/10.1016/j.checat.2022.08.018.
[42] D.J.D. Pimlott, A. Jewlal, B.A.W. Mowbray, C.P. Berlinguette, Impurity-Resistant CO_2 Reduction Using Reactive Carbon Solutions, ACS Energy Lett. 8 (2023) 1779–1784, https://doi.org/10.1021/acsenergylett.3c00133.
[43] J. Leverett, J.A. Yuwono, P. Kumar, T. Tran-Phu, J. Qu, J. Cairney, X. Wang, A. N. Simonov, R.K. Hocking, B. Johannessen, L. Dai, R. Daiyan, R. Amal, Impurity tolerance of unsaturated Ni-N-C active sites for practical electrochemical CO_2 reduction, ACS Energy Lett. 7 (2022) 920–928, https://doi.org/10.1021/acsenergylett.1c02711.
[44] T. Al-Attas, S.K. Nabil, A.S. Zeraati, H.S. Shiran, T. Alkayyali, M. Zargartalebi, T. Tran, N.N. Marei, M.A. Al Bari, H. Lin, S. Roy, P.M. Ajayan, D. Sinton, G. Shimizu, M.G. Kibria, Permselective MOF-based gas diffusion electrode for direct conversion of CO_2 from quasi flue gas, ACS Energy Lett. 8 (2023) 107–115, https://doi.org/10.1021/acsenergylett.2c02305.
[45] P. Karimi, A. Alihosseinzadeh, S. Ponnurangam, K. Karan, Performance characteristics of polymer electrolyte membrane CO_2 electrolyzer: effect of CO_2 dilution, flow rate and pressure, J. Electrochem. Soc. 169 (2022) 064510, https://doi.org/10.1149/1945-7111/ac725f.
[46] X. Zhang, Z. Wang, Z. Chen, Y. Zhu, Z. Liu, F. Li, W. Zhou, Z. Dong, J. Fan, L. Liu, Molecular trapdoor mechanism of In-SSZ-13(MP) holds promise for selective electrochemical reduction of CO_2 at low concentrations, Appl. Catal. B: Environ. 317 (2022) 121771, https://doi.org/10.1016/j.apcatb.2022.121771.
[47] B. Xiong, J. Liu, Y. Yang, Y. Yang, Z. Hua, Effect mechanism of NO on electrocatalytic reduction of CO_2 to CO over Pd@Cu bimetal catalysts, Fuel 323 (2022) 124339, https://doi.org/10.1016/j.fuel.2022.124339.
[48] A. Anzai, M. Higashi, M. Yamauchi, Direct electrochemical CO_2 conversion using oxygen-mixed gas on a Cu network cathode and tailored anode, Chem. Commun. 59 (2023) 11188–11191, https://doi.org/10.1039/D3CC03298A.
[49] S.K. Nabil, S. Roy, W.A. Algozeeb, T. Al-Attas, M.A. Al Bari, A.S. Zeraati, K. Kannimuthu, P.G. Demingos, A. Rao, T.N. Tran, X. Wu, P. Bollini, H. Lin, C. V. Singh, J.M. Tour, P.M. Ajayan, M.G. Kibria, Bifunctional gas diffusion electrode enables in situ separation and conversion of CO_2 to ethylene from dilute stream, Adv. Mater. 35 (2023) 2300389, https://doi.org/10.1002/adma.202300389.
[50] M. He, C. Li, H. Zhang, X. Chang, J.G. Chen, W.A. Goddard, M. jeng Cheng, B. Xu, Q. Lu, Oxygen induced promotion of electrochemical reduction of CO_2 via co-electrolysis, Nat. Commun. 11 (2020) 3844, https://doi.org/10.1038/s41467-020-17690-8.
[51] M. Moradzaman, C.S. Martínez, G. Mul, Effect of partial pressure on product selectivity in Cu-catalyzed electrochemical reduction of CO_2, Sustain. Energy Fuels 4 (2020) 5195–5202, https://doi.org/10.1039/d0se00865f.
[52] M.M. Halmann, M. Steinberg, M. Gattrell, N. Gupta, A. Co, Effect of gaseous impurities on the electrochemical reduction of CO_2 on copper electrodes, ECS Trans. 19 (2009) 1–13. DOI 10.1149/1.3220175.
[53] X. Wang, F. Li, W.-J. Yin, Y. Si, M. Miao, X. Wang, Y. Fu, Atomically dispersed Sn modified with trace sulfur species derived from organosulfide complex for electroreduction of CO_2, Appl. Catal. B: Environ. 304 (2022) 120936, https://doi.org/10.1016/j.apcatb.2021.120936.
[54] I. Grigioni, L.K. Sagar, Y.C. Li, G. Lee, Y. Yan, K. Bertens, R.K. Miao, X. Wang, J. Abed, D.H. Won, F.P. Garciá De Arquer, A.H. Ip, D. Sinton, E.H. Sargent, CO_2 electroreduction to formate at a partial current density of 930 mA cm_{-2} with InP colloidal quantum dot derived catalysts, ACS Energy Lett. 6 (2020) 79–84, https://doi.org/10.1021/acsenergylett.0c02165.
[55] B. Ávila-Bolívar, V. Montiel, J. Solla-Gullón, On the activity and stability of Sb2O3/Sb nanoparticles for the electroreduction of CO_2 toward formate, J. Electroanal. Chem. 895 (2021) 115440, https://doi.org/10.1016/j.jelechem.2021.115440.
[56] C. Xia, P. Zhu, Q. Jiang, Y. Pan, W. Liang, E. Stavitsk, Continuous production of pure liquid fuel solutions via electrocatalytic CO_2 reduction using solid-electrolyte devices, Nat. Energy 4 (2019) 776–785, https://doi.org/10.1038/s41560-019-0451-x.
[57] L. Li, A. Ozden, S. Guo, F.P. García de Arquer, C. Wang, M. Zhang, J. Zhang, H. Jiang, W. Wang, H. Dong, D. Sinton, E.H. Sargent, M. Zhong, Stable, active CO_2 reduction to formate via redox-modulated stabilization of active sites, Nat. Commun. 12 (2021) 5223, https://doi.org/10.1038/s41467-021-25573-9.
[58] B. Ávila-Bolívar, L. García-Cruz, V. Montiel, J. Solla-Gullón, Electrochemical reduction of CO_2 to formate on easily prepared carbon-supported Bi nanoparticles, Molecules 24 (2019) 2032, https://doi.org/10.3390/molecules24112032.
[59] J.A. Abarca, G. Díaz-Sainz, I. Merino-Garcia, G. Beobide, J. Albo, A. Irabien, Optimized manufacturing of gas diffusion electrodes for CO_2 electroreduction with automatic spray pyrolysis, J. Environ. Chem. Eng. 11 (2023) 109724, https://doi.org/10.1016/j.jece.2023.109724.
[60] G. Díaz-Sainz, M. Alvarez-Guerra, J. Solla-Gullón, L. García-Cruz, V. Montiel, A. Irabien, CO_2 electroreduction to formate: continuous single-pass operation in a filter-press reactor at high current densities using Bi gas diffusion electrodes, J. CO_2 Util. 34 (2019) 12–19, https://doi.org/10.1016/j.jcou.2019.05.035.
[61] G. Díaz-Sainz, K. Fernández-Caso, T. Lagarteira, S. Delgado, M. Alvarez-Guerra, A. Mendes, A. Irabien, Coupling continuous CO_2 electroreduction to formate with efficient Ni-based anodes, J. Environ. Chem. Eng. 11 (2023) 109171, https://doi.org/10.1016/j.jece.2022.109171.
[62] X. Ge, A. Sumboja, D. Wuu, T. An, B. Li, F.W.T. Goh, T.S.A. Hor, Y. Zong, Z. Liu, Oxygen reduction in alkaline media: from mechanisms to recent advances of catalysts, ACS Catal. 5 (2015) 4643–4667, https://doi.org/10.1021/acscatal.5b00524.